Control of Self-Assembly by Charge-Transfer Complexation between C_{60} Fullerene and Electron Donating Units of Block Copolymers

Ari Laiho,[†] Robin H. A. Ras,[†] Sami Valkama,[†] Janne Ruokolainen,[†] Ronald Österbacka,[‡] and Olli Ikkala*[,†]

Department of Engineering Physics and Mathematics and Center for New Materials, Helsinki University of Technology, P.O. Box 2200, FI-02015 HUT, Espoo, Finland, and Department of Physics, Åbo Akademi University, Porthansgatan 3, Turku 20500, Finland

Received May 23, 2006; Revised Manuscript Received August 25, 2006

ABSTRACT: Self-assembly allows new opportunities to control the morphology and properties of fullerene-based materials. By using the electron-accepting underivatized C_{60} and electron-donating pyridine groups of a polystyrene-*block*-poly(4-vinylpyridine), PS-*block*-P4VP, we here show the first example that charge-transfer complexation between fullerenes and block copolymers can essentially modify the self-assembled structures. The morphology of C_{60}/PS-*block*-P4VP mixture is studied in both bulk and thin films by transmission electron microscopy (TEM) and small-angle X-ray scattering (SAXS) upon casting from freshly prepared or differently aged xylene solutions. Selecting PS-*block*-P4VP that leads to hexagonal self-assembly with P4VP cylindrical cores, closely similar cylindrical structure is observed upon adding a small amount of C_{60}, when freshly prepared xylene solutions are used to cast solid bulk or thin film samples. In this case the C_{60} molecules swell the PS matrix. By contrast, spherical morphology is observed if aged xylene solutions have been used where C_{60} has slowly penetrated into the P4VP micellar cores due to charge-transfer complexation, as evidenced by UV−vis and FTIR spectroscopy. This morphological change is unexpected, as according to simple block copolymer theory selective incorporation of a small molecular species or nanoparticles within the minority block of hexagonally self-assembled cylindrical diblock copolymer system should render the morphology toward lamellar structures. This suggests that charge-transfer complexation can be relevant in considering the self-assembled structures of block copolymers and fullerenes.

Introduction

Block copolymers[1−3] and fullerenes[4−6] are among the important building blocks for functional nanostructured materials. Block copolymers are constituted of well-defined mutually repulsive polymeric blocks that are covalently connected, thus leading to competing interactions and therefore self-assembly. Tailoring of the blocks and architectures allows control of the nanoscale structures and tuning of the phase transitions for various applications.[1−3,7,8] Complementary physical interactions, which are dealt in supramolecular chemistry,[9] can be applied to block copolymers to achieve further levels of structures and hierarchies and to prepare discrete nanoscale objects.[10−12] Important to the present context is that also the assembly of nanoparticles can be controlled by block copolymers leading to new structures and properties.[13−16] C_{60} fullerenes are ca. 1 nm spherical carbon-based molecules that have attracted large attention because of their interesting electronic, magnetic, and optical properties.[4−6,17−20] Various derivatives have been synthesized to improve the solubility, to control the assembly, and to provide further functionalities.[6,21−24] There have been several efforts to combine fullerenes and block copolymeric self-assembly, in an effort to control the aggregation and to achieve functional properties.[25−27] Polymer brushes have been attached onto fullerenes,[28,29] which provide compatibility in selected domains of self-assembled block copolymers.[27] Furthermore, fullerenes have been connected to specific blocks of block copolymers using covalent interactions[30−34] or even using complementary physical interactions, such as acid−base interactions[35] and hydrogen bonding.[25] A recent example of the latter case is based on carboxylic acid-derivatized fullerenes which selectively bond to the basic pyridine groups of polystyrene-*block*-poly(4-vinylpyridine) (PS-*block*-P4VP), thus modifying the self-assembled structures.[25]

In the present work we demonstrate a particularly facile method for self-assembling underivatized fullerenes based on mixtures with PS-*block*-P4VP block copolymers and show that charge-transfer complexation can have an essential effect on the self-assembled structure (Scheme 1). Upon swelling of C_{60} within the P4VP domains, one could a priori expect morphological changes analogous to the diblock copolymer structures corresponding to larger effective volume fraction of P4VP, as demonstrated using mixtures of PS-*block*-P4VP block copolymer with CdS nanoparticles[36] or surfactant.[37] By contrast, in the present case the morphological shift is to the opposite direction. Our findings show that charge-transfer complexation must be taken into consideration in analyzing the self-assembled structures of C_{60} and block copolymers containing electron-donating groups.

Experimental Section

Materials and Sample Preparation. Polystyrene-*block*-poly(4-vinylpyridine) (PS-*block*-P4VP) diblock copolymer was obtained from Polymer Source Inc. and C_{60} (98%) from Aldrich, and they were used without further purification. A range of block lengths were used (see the Supporting Information), but PS-*block*-P4VP with molecular weights of 47 600 and 20 900 g/mol for the PS and P4VP blocks, respectively, with polydispersity of $M_w/M_n = 1.14$, showed a feasible solubility in xylene, still having a relatively long P4VP block needed for self-assembly. Xylene (98%, mixture of isomers, LabScan) and pyridine (>99.8%, Fluka) were used as received. First, micellar solutions of PS-*block*-P4VP in xylene were prepared. C_{60} was separately dissolved in xylene using sonication

[†] Helsinki University of Technology.
[‡] Åbo Akademi University.
* Corresponding author: Tel +358-50-4100454; Fax +358-9-4513155; e-mail olli.ikkala@tkk.fi.

10.1021/ma061165g CCC: $33.50
Published on Web 09/28/2006

Scheme 1. Schematic Illustration of the Charge-Transfer Complexation between PS-*block*-P4VP and C_{60}

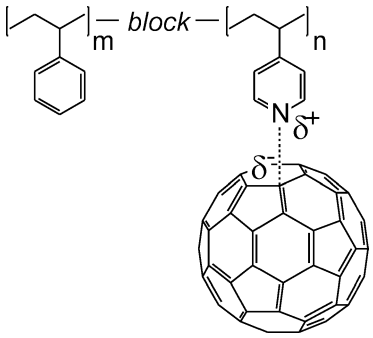

(concentration < 0.3 wt %); thereafter, the polymer solution was mixed with the C_{60} solution, and the obtained solution (final polymer concentration = 1.4 wt %) was further sonicated. Thereafter, the solvent was slowly evaporated at room temperature or the solutions were spin-cast at 1000 rpm onto NaCl substrates (Sigma-Aldrich, IR crystal window) in order to prepare bulk or thin film samples, respectively. The spin-cast films were dried under vacuum (ca. 10^{-3} mbar) at 30 °C for 24 h followed by annealing under high vacuum (ca. 10^{-6} mbar) at 170 °C for 3 days. The same thermal treatment was performed for bulk samples, except that the annealing was done at 210 °C.

Ultraviolet−Visible (UV−Vis) Spectroscopy. UV−vis spectra of the solutions were measured using a Perkin-Elmer Lambda 900 spectrometer. Standard quartz cuvettes with a path length of 2 mm were used.

Infrared Spectroscopy. Infrared spectra were obtained using a Nicolet 750 FTIR spectrometer. Samples were prepared by drop-casting onto potassium bromide substrates.

Transmission Electron Microscopy (TEM). The spin-cast films were separated from the NaCl substrates by dipping the substrate into water, thus leaving the films on the water surface where they were picked up onto 600-mesh copper grids. Thin films were also picked up onto an epoxy piece and further embedded in epoxy in order to obtain cross-sectional images of the thin films. Embedded thin films and bulk samples were microtomed at room temperature using a Leica Ultracut UCT-ultramicrotome and a Diatome diamond knife to yield sections of ~60 nm in thickness. Both thin film and bulk samples were stained in I_2 vapor for 4 h in order to improve contrast. Bright-field TEM was performed on a FEI Tecnai 12 transmission electron microscope operating at an accelerating voltage of 120 kV.

Small-Angle X-ray Scattering (SAXS). X-ray scattering patterns were collected using a Bruker SAXS system that includes a 2-D area detector (Bruker AXS). The generator is a Bruker MICROSTAR rotating anode X-ray source with Montel Optics (Cu Kα radiation λ = 1.54 Å), and it was operated at 45 kV and 60 mA. The X-ray beam was further collimated with four sets of 4-blade slits. The sample-to-detector distance was ~2.5 m. The magnitude of the scattering vector is given by $q = (4\pi/\lambda) \sin \theta$, where 2θ is the scattering angle and the q range was calibrated with a rat-tail collagen standard.

Results and Discussion

Solution Behavior. We first discuss the solution properties using UV−vis spectroscopy. C_{60} dissolves readily in xylene, which leads to a purple solution, where the UV−vis spectrum shows a broad and only weakly structured absorption band ranging from ca. 450 to 650 nm (see the Supporting Information). Also, when pyridine is used as a solvent for C_{60}, then the spectrum initially resembles that of C_{60} dissolved in xylene. Upon aging, however, the color of the C_{60}/pyridine solution changes from purple to brown, which manifests in the UV−vis spectra as an increase in absorbance in the region 450−550 nm (see the inset in Figure 1). Such an observation agrees with the

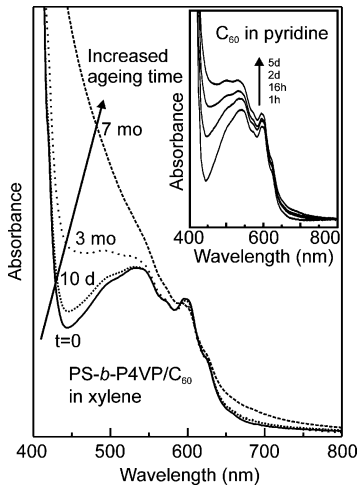

Figure 1. UV−vis spectra at different aging times for PS-*block*-P4VP/C_{60} (95/5 w/w) dissolved in xylene (polymer concentration is 1.4 wt %). The spectra are shown for a freshly prepared purple solution as well as for the aging times of 10 days, 3 months, and 7 months, leading to brown solutions. The inset shows the spectra for C_{60} dissolved in pyridine solvent at concentration of 0.1 wt %. The aging times in this case are 1 h, 16 h, 2 days, and 5 days.

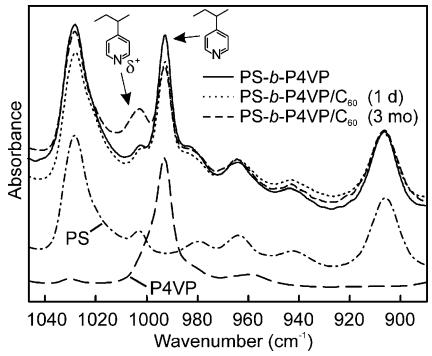

Figure 2. FTIR spectra for P4VP, PS, PS-*block*-P4VP, and PS-*block*-P4VP/C_{60} (95/5 w/w) for the aging times 1 day and 3 months.

formation of charge-transfer complexes between the electron-donating pyridine solvent and the electron-accepting fullerenes.[38−41] Next, polymers are added to the compositions. A binary mixture of C_{60}/xylene and a ternary mixture consisting of PS/C_{60} 95/5 w/w in xylene show roughly similar absorption spectra, and they do not change notably even during an aging time of 8 months (see the Supporting Information). However, the situation is different if PS-*block*-P4VP/C_{60} (95/5 w/w) is dissolved in xylene. The freshly prepared solution is purple, and its absorption spectrum is qualitatively similar to that of PS/C_{60} in xylene (Figure 1). Upon aging, the absorbance in the region ca. 450−550 nm increases, and the solution becomes brown, similar to the solutions of C_{60} in pyridine. Formation of large aggregates which would scatter light only in the blue part of the visible spectrum can be excluded on the basis of dynamic light scattering experiments (see the Supporting Information) which show only block copolymer micelles. The increased absorbance in aged samples is thus due to charge-transfer complexation between C_{60} and the pyridine units of the block copolymer.

FTIR spectroscopy provides further evidence for the complexation. Upon aging of C_{60}/PS-*block*-P4VP, the pyridine band at 993 cm^{-1} is slightly but reproducibly decreased, and a new band appears at 1003 cm^{-1} (Figure 2). This suggests that in aged samples partial charging of the pyridine units is created, obviously due to charge transfer. Importantly, related shifts in the 993 cm^{-1} bands have been reported for hydrogen-bonding

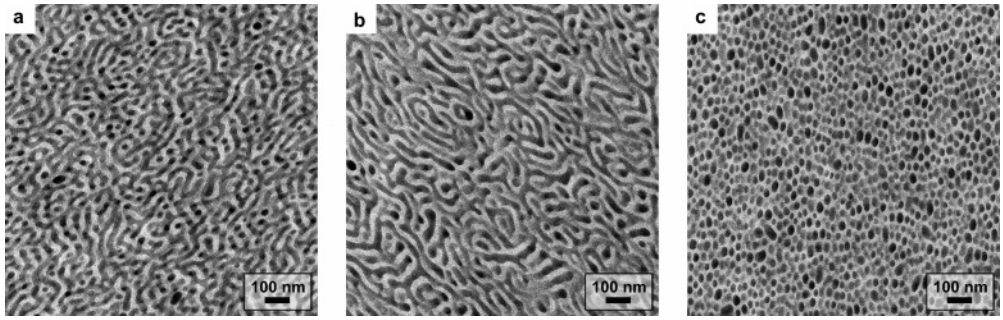

Figure 3. TEM images of annealed bulk samples after evaporation of xylene: (a) pure PS-*block*-P4VP, (b) PS-*block*-P4VP/C_{60} (95/5 w/w) prepared from a fresh purple xylene solution, and (c) PS-*block*-P4VP/C_{60} (95/5 w/w) prepared from an aged 3 months old brown xylene solution. The samples have been stained in I_2 vapor.

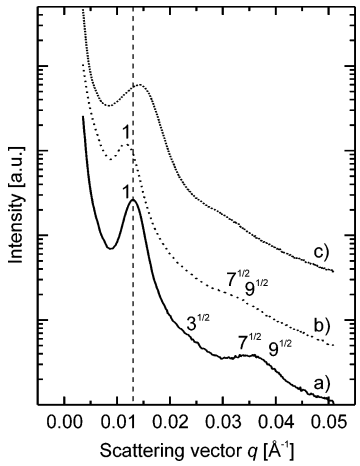

Figure 4. SAXS intensity patterns of annealed bulk samples after evaporation of xylene: (a) pure PS-*block*-P4VP, (b) PS-*block*-P4VP/C_{60} (95/5 w/w) prepared from a fresh purple xylene solution, and (c) PS-*block*-P4VP/C_{60} (95/5 w/w) prepared from an aged 3 months old brown xylene solution.

interactions.[42] Note that also PS has a weak absorption band near 1003 cm^{-1}, overlapping with the pyridinium band. The observation that the band shift is partial means that only part of the pyridine units have interacted with C_{60}, which is likely. The most characteristic band for interactions of pyridine[43] near 1600 cm^{-1} could not be used for interpretation because of the strongly overlapping aromatic carbon−carbon stretching vibration of the phenyl groups of PS. Furthermore, homopolymeric P4VP was not an option because no common solvent could be found for the P4VP homopolymer and C_{60}.

In summary, the behavior of the above C_{60}/PS-*block*-P4VP composition in xylene solution can be understood on the basis of UV−vis and FTIR spectroscopic data, combined with the earlier reports on charge-transfer interaction between C_{60} and pyridine solvent.[38−41] In freshly prepared samples, the C_{60} molecules are essentially not found in the P4VP cores of the PS-*block*-P4VP micelles due to the compatibility of C_{60}, PS blocks, and xylene, whereas upon aging the C_{60} molecules slowly penetrate into the micellar cores to form charge-transfer complexes, as schematically illustrated in Scheme 1.

Bulk Morphology. Next, we consider the bulk morphology of the above PS-*block*-P4VP/C_{60} mixtures after solvent removal. To dissolve PS-*block*-P4VP in xylene which is a favored solvent for C_{60}, the PS block must be sufficiently long with respect to the P4VP block, and this puts restrictions to the useful block lengths. The PS and P4VP block lengths 47 600 and 20 900 g/mol turned out to be particularly feasible. In the annealed bulk state, such block lengths have been previously reported to self-assemble into a hexagonally arranged cylindrical morphology based on TEM and SAXS,[36] which is not unexpected as the P4VP weight fraction is 0.31. Figure 3a shows a TEM image of the pure PS-*block*-P4VP, which indeed suggests a cylindrical morphology consisting of P4VP cylinders in the PS matrix, where the structure, however, remains relatively poor as the sample has not been aligned. The hexagonal packing should lead to the relative positions of the Bragg peaks q_{hk} at $q_{hk}/q_{10} = \sqrt{h^2+hk+k^2}$, where $h, k \in \{0, 1, 2, ...\}$ and q_{10} is the position of the first Bragg peak. The observed SAXS intensity pattern (Figure 4) shows the first Bragg peak at q_{10}, a faint reflection at $\sqrt{3}q_{10}$, and a broad combination of $\sqrt{7}q_{10}$ and $3q_{10}$ reflections, whereas the reflection at $q_{20} = 2q_{10}$ is not seen most probably because it is coincident with a minimum in the form factor of the cylinders. If 5 wt % of C_{60} is added to the system, the hexagonally arranged structure is still observed in samples

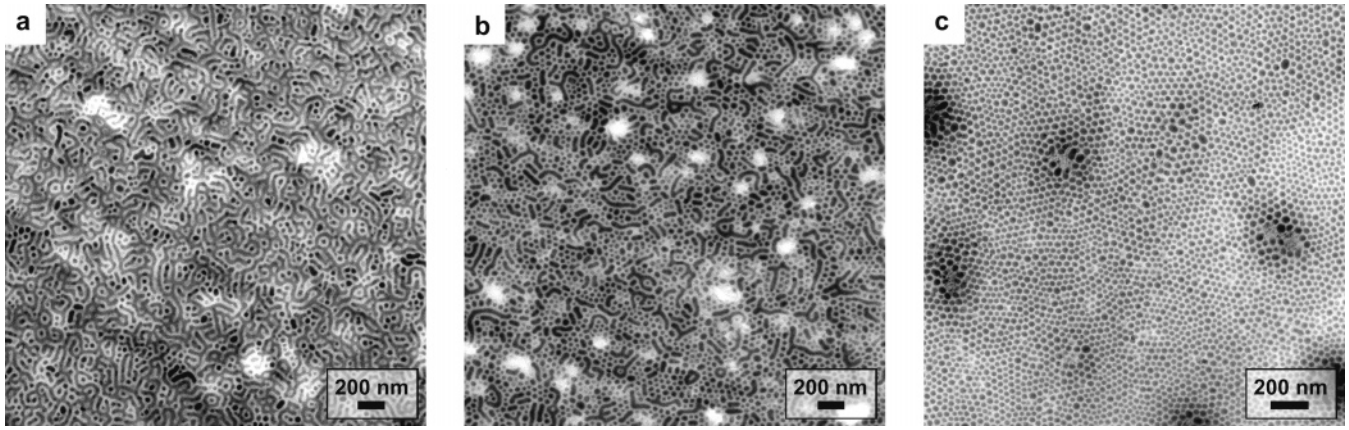

Figure 5. TEM images of ~50 nm thick spin-cast annealed thin films: (a) pure PS-*block*-P4VP, (b) PS-*block*-P4VP/C_{60} (95/5 w/w) prepared from a fresh purple xylene solution, and (c) PS-*block*-P4VP/C_{60} (95/5 w/w) prepared from an aged 3 months old brown xylene solution. The samples have been stained in I_2 vapor.

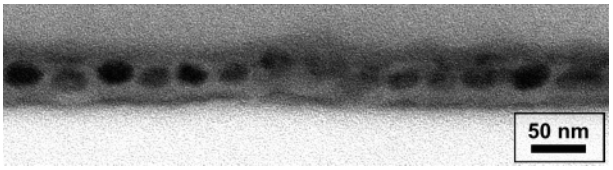

Figure 6. Cross-sectional TEM image of a thin film spin-cast from an aged 3 months old brown PS-*block*-P4VP/C_{60} 96/4 w/w solution confirming the presence of spheres.

cast from fresh xylene solutions based on TEM (see Figure 3b), but SAXS shows (Figure 4) that the long period $L_p = 2\pi/q_{10}$ increases from 48 to 54 nm. By contrast, if an aged xylene solution of PS-*block*-P4VP/C_{60} is used for casting the sample, TEM shows a remarkable morphological change from P4VP containing cylinders to P4VP containing spheres. In a later section, arguments are given that in this morphological change at least part of the C_{60} molecules leave the PS matrix and enter in the P4VP domains due to charge-transfer complexation. Also, SAXS suggests morphological change, even if the higher order peaks are broad. A decrease in the long period from 54 to 45 nm occurs based on the main reflection (Figure 4).

Thin Film Morphology. Similar morphological change as in bulk was observed also in 50 nm thin films, as can be seen in the TEM images in Figure 5a−c. Films spin-cast from freshly prepared xylene solutions of PS-*block*-P4VP/C_{60} 95/5 w/w render a structure (Figure 5b) that is qualitatively similar to that of the pure PS-*block*-P4VP (Figure 5a), i.e., a cylindrical structure with a fraction of spheres. A closer investigation reveals that the amount of cylinders has slightly decreased whereas that of spheres has increased, in agreement with an increase in the relative volume of the PS matrix. The diameter of the cylinders seems to remain constant at around 25 nm upon addition of C_{60}. Interestingly, the film morphology changes to purely spherical if aged PS-*block*-P4VP/C_{60} 95/5 w/w solutions are used for spin-casting (Figure 5c), as was also observed in bulk samples. The cross-sectional TEM image of such a film (Figure 6) excludes the possibility of upright cylinders and verifies the spherical morphology. Furthermore, based on TEM the diameter of the spheres seems to be slightly larger than that of the cylinders of the pure block copolymer thin film. The C_{60}-containing P4VP spheres pack into a relatively well ordered hexagonal array in a thin film, whereas only a poor arrangement was seen in bulk. The difference in packing is probably due to the spatial constraint between the air−film and film−substrate interface.

Influence of the Charge-Transfer Complexation on the Morphology. Next, we discuss potential reasons for the observed morphological changes in PS-*block*-P4VP/C_{60} mixtures from cylinders (prepared from fresh xylene solutions) to spheres (prepared from aged xylene solutions) in both bulk and thin films. Within the used concentrations (1.4 wt %), PS-*block*-P4VP forms spherical micelles in xylene solutions with PS corona and P4VP cores because xylene is a poor solvent for P4VP, and it is thus expelled from the xylene. Therefore, as expected from the solubility of C_{60} in xylene, in the freshly prepared xylene solutions of C_{60} and PS-*block*-P4VP the C_{60} molecules are predominantly found in the PS domains and not in the P4VP micellar cores. This is supported by the UV−vis spectra (Figure 1). Accordingly, spin-casting or solvent-casting from fresh solutions should lead to swelling of the PS matrix compared to pure block copolymer, and this is in fact confirmed by the TEM (Figure 3b for bulk and Figure 5b for films) and SAXS (Figure 4) where increase in the spacing of adjacent cylinders is observed in bulk and a trend toward spheres is observable in thin films. Upon aging, the UV−vis spectra of the xylene mixtures of PS-*block*-P4VP/C_{60} (95/5 w/w) slowly become similar to that of pure C_{60} dissolved in pyridine solvent (Figure 1), i.e., the spectra show interaction between the pyridines and C_{60} molecules. This suggests that, with time, part of the C_{60} molecules penetrate into the P4VP cores of the PS-

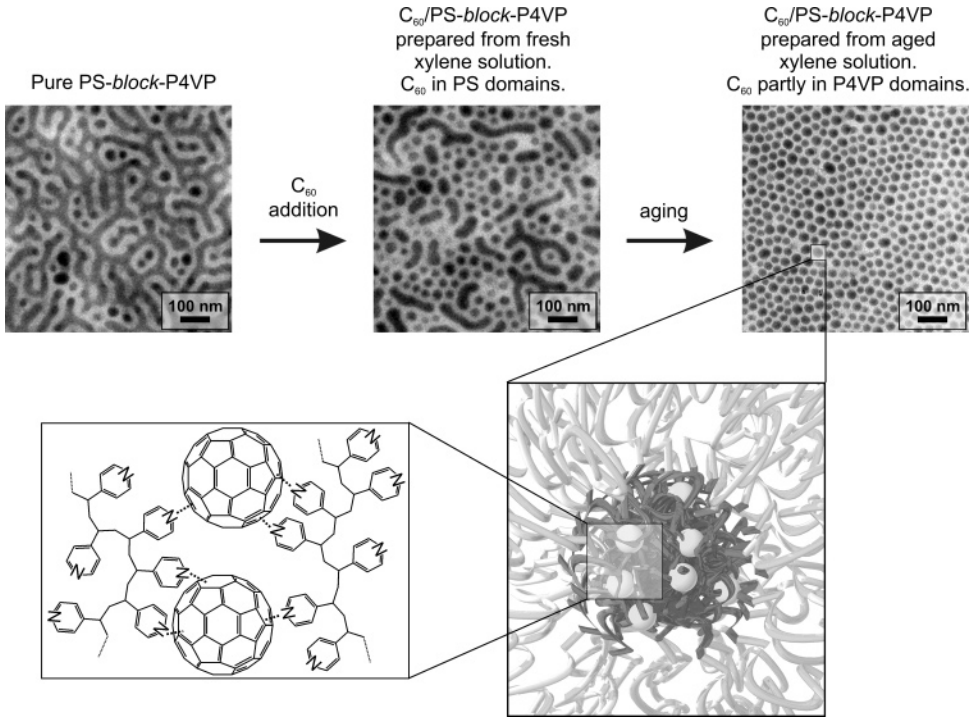

Figure 7. Schematic representation of the self-assembled PS-*block*-P4VP/C_{60} structures formed through charge-transfer complexation with the pyridines. The TEM micrographs are enlargements of Figure 5a−c. The strong tendency of C_{60} molecules to aggregate combined with the possibility that each C_{60} molecule can bind multiple P4VP chains together through charge transfer is suggested to cause the morphological change from P4VP cylinders to C_{60}-containing P4VP spheres.

block-P4VP micelles and form charge-transfer complexes with pyridines (Scheme 1). Spherical structures were observed when prepared from aged xylene solutions instead of the cylindrical structures as prepared from fresh solutions. During aging of the xylene solution of C_{60}/PS-*block*-P4VP, part of the C_{60} molecules move from the majority PS domains to the minority P4VP domains due to charge-transfer complexes, and therefore the effective volume fraction of the P4VP-rich domain increases in relation to that of PS. According to simple diblock copolymer models,[3] addition of small compatible species to P4VP domain should render structures toward lamellar P4VP domains and not to the opposite direction, i.e., spherical P4VP domains, as is experimentally observed in the above PS-*block*-P4VP/C_{60} system.

The influence of nanoparticles on the phase behavior of diblock copolymers has been investigated using Monte Carlo simulations and theoretical models.[15,44−46] Consistent with the theory, an expected change from a cylindrical to a lamellar bulk structure was observed upon addition of CdS nanoparticles into the P4VP domains using a PS-*block*-P4VP block copolymer with similar molecular weights as in the present work.[36] Analogous observations have been made also in systems where surfactant-like molecules are hydrogen bonded to the P4VP blocks of PS-*block*-P4VP, i.e., where the surfactant-like molecules effectively increase the volume fraction of the P4VP-rich domains, leading to structural changes that can be understood by simple diblock copolymer models.[37]

In the present work, by contrast, incorporation of C_{60} within the P4VP domains when using aged solutions leads to cylindrical to spherical morphological change in bulk or in thin films. We suggest that the main reason for this morphological change can be attributed to C_{60} forming charge-transfer complexes with multiple pyridine groups from different block copolymer chains. On the basis of the spectroscopic evidence, C_{60} forms charge-transfer complexes with the pyridines of the PS-*block*-P4VP block copolymer. As C_{60} can theoretically accept up to six electrons and thus interact simultaneously with up to six pyridine groups, each C_{60} molecule can bind several P4VP chains together via charge-transfer interaction. Such multiple interactions combined with the strong tendency of C_{60} molecules to aggregate render the morphology toward spherical structures even though the volume fraction of P4VP domain increases, and the theories would suggest a change toward lamellar morphology. This is schematically summarized in Figure 7.

Related morphological change but due to different types of interactions and materials has been reported in polystyrene-*block*-poly(ethylene oxide) (PS-*block*-PEO) block copolymer thin films upon addition of cadmium sulfide (CdS) nanoparticles.[47] They reported that the morphological change of PEO cylinders into CdS/PEO spheres was due to the presence of multiple hydrogen bonds between surface-hydroxylated CdS nanoparticles and PEO. Recently, carboxylic acid-functionalized C_{60} molecules were hydrogen bonded to the pyridine groups of PS-*block*-P4VP, and spherical morphologies of the micelles were observed.[25] An explanation was suggested that the underlying mechanism could be due to formation of hydrogen bonds between pyridine and C_{60}-COOH. Our present work suggests that charge-transfer complexation could have played a role also in their work, in particular as the characteristic color change to brown was reported also in their case.[25] We demonstrate that underivatized C_{60} without additional functional groups is able to interact with block copolymers and can control the self-assembly via charge-transfer complexation.

Conclusion

We have demonstrated that C_{60}/block copolymer systems can lead to unexpected self-assembled structures in both bulk and spin-cast films, if the block copolymer contains electron-donating moieties that form charge-transfer complexes with the electron-accepting C_{60} molecules. Such effects were here demonstrated using mixtures of C_{60} and PS-*block*-P4VP. Upon aging of the solutions, spectroscopy revealed formation of charge-transfer complexes between pyridine and C_{60}, which lead to preference of spherical self-assembled structures as evidenced by TEM and SAXS. The strong tendency of C_{60} to aggregate combined with the fact that one C_{60} molecule can bind multiple P4VP chains together through charge transfer is suggested to cause the morphological change. We foresee that charge-transfer complexation becomes essential to understand some of the self-assembled structures of C_{60}, and they can, when used in a rational way, lead to novel pathways for the construction of self-assembled fullerene containing materials and tuning of the functions.

Acknowledgment. This work has been supported by grants from the National Technology Agency of Finland and the Academy of Finland. The work has been performed within the Centre of Excellence of Bio- and Nanopolymers (77317) of the Academy of Finland. Dr. Harri Kosonen (TKK) and Dr. Himadri Majumdar (ÅA) are acknowledged for several discussions and Susanna Holappa (TKK) and Prof. Janne Laine (TKK) for assistance with the DLS measurements.

Supporting Information Available: Table for the used PS-*block*-P4VP molecular weights, UV−vis spectroscopic data for PS-*block*-P4VP, C_{60}, PS/C_{60}, and PS-*block*-P4VP/C_{60} in xylene, TEM images of PS-*block*-P4VP thin films, and DLS data for PS-*block*-P4VP and PS-*block*-P4VP/C_{60} mixture in xylene. This material is available free of charge via the Internet at http://pubs.acs.org.

References and Notes

(1) Bates, F. S.; Fredrickson, G. H. *Phys. Today* **1999**, *52*, 32−38.
(2) Hadjichristidis, N.; Pispas, S.; Floudas, G. *Block Copolymers: Synthetic Strategies, Physical Properties, and Applications*; Wiley: New York, 2002.
(3) Hamley, I. W. *The Physics of Block Copolymers;* Oxford University Press: Oxford, 1998.
(4) Kroto, H. W.; Heath, J. R.; O'Brien, S. C.; Curl, R. F.; Smalley, R. E. *Nature (London)* **1985**, *318*, 162−163.
(5) Taylor, R.; Walton, D. R. *Nature (London)* **1993**, *363*, 685−693.
(6) Wudl, F. *J. Mater. Chem.* **2002**, *12*, 1959−1963.
(7) Abetz, V. *Assemblies in Complex Block Copolymer Systems*; Marcel Dekker: New York, 2000; pp 215−262.
(8) Hamley, I. W. *Angew. Chem., Int. Ed.* **2003**, *42*, 1692−1712.
(9) Lehn, J.-M. *Supramolecular Chemistry;* VCH: Weinheim, 1995.
(10) Antonietti, M. *Nat. Mater.* **2003**, *2*, 9−10.
(11) Ikkala, O.; ten Brinke, G. *Chem. Commun.* **2004**, 2131−2137.
(12) Ruokolainen, J.; Mäkinen, R.; Torkkeli, M.; Mäkelä, T.; Serimaa, R.; ten Brinke, G.; Ikkala, O. *Science* **1998**, *280*, 557−560.
(13) Fink, Y.; Urbas, A. M.; Bawendi, M. G.; Joannopoulos, J. D.; Thomas, E. L. *J. Lightwave Technol.* **1999**, *17*, 1963−1969.
(14) Lee, J. Y.; Shou, Z.; Balazs, A. C. *Macromolecules* **2003**, *36*, 7730−7739.
(15) Lee, J. Y.; Thompson, R. B.; Jasnow, D.; Balazs, A. C. *Macromolecules* **2002**, *35*, 4855−4858.
(16) Lin, Y.; Böker, A.; He, J.; Sill, K.; Xiang, H.; Abetz, C.; Li, X.; Wang, J.; Emrick, T.; Long, S.; Wang, Q.; Balazs, A. C.; Russell, T. P. *Nature (London)* **2005**, *434*, 55−59.
(17) Dresselhaus, M. S.; Dresselhaus, G.; Eklund, P. C. *J. Mater. Res.* **1993**, *8*, 2054−2097.
(18) Haddon, R. C. *Nature (London)* **1995**, *378*, 249−255.
(19) Hirsch, A. *Top. Curr. Chem.* **1999**, *199*, 1−65.
(20) Knupfer, M. *Surf. Sci. Rep.* **2001**, 42, *1*−74.
(21) Geckeler, K. E.; Samal, S. *Polym. Int.* **1999**, *48*, 743−757.
(22) Mignard, E.; Hiorns, R. C.; Francois, B. *Macromolecules* **2002**, *35*, 6132−6141.

(23) Prato, M. *J. Mater. Chem.* **1997**, *7*, 1097−1109.
(24) Wang, C.; Guo, Z.-X.; Fu, S.; Wu, W.; Zhu, D. *Prog. Polym. Sci.* **2004**, *29*, 1079−1141.
(25) Fujita, N.; Yamashita, T.; Asai, M.; Shinkai, S. *Angew. Chem., Int. Ed.* **2005**, *44*, 1257−1261.
(26) Jenekhe, S. A.; Chen, X. L. *Science* **1998**, *279*, 1903−1907.
(27) Schmaltz, B.; Brinkmann, M.; Mathis, C. *Macromolecules* **2004**, *37*, 9056−9063.
(28) Ederle, Y.; Mathis, C. *Macromolecules* **1997**, *30*, 2546−2555.
(29) Samulski, E. T.; DeSimone, J. M.; Hunt, M. O.; Menceloglu, Y. Z.; Jarnagin, R. C.; York, G. A.; Labat, K. B.; Wang, H. *Chem. Mater.* **1992**, *4*, 1153−1157.
(30) Stalmach, U.; de Boer, B.; Videlot, C.; van Hutten, P. F.; Hadziioannou, G. *J. Am. Chem. Soc.* **2000**, *122*, 5464−5472.
(31) Hadziioannou, G. *MRS Bull.* **2002**, *27*, 456−460.
(32) Nierengarten, J.-F.; Guttierez-Nava, M.; Zhang, S.; Masson, P.; Oswald, L.; Bourgogne, C.; Rio, Y.; Accorsi, G.; Armaroli, N.; Setayesh, S. *Carbon* **2004**, *42*, 1077−1083.
(33) Ball, Z. T.; Sivula, K.; Frechet, J. M. J. *Macromolecules* **2006**, *39*, 70−72.
(34) Sivula, K.; Ball, Z. T.; Watanabe, N.; Frechet, J. M. J. *Adv. Mater.* **2006**, *18*, 206−210.
(35) Huang, X.-D.; Goh, S. H.; Lee, S. Y.; Huan, C. H. A. *Macromol. Chem. Phys.* **2000**, *201*, 281−287.
(36) Yeh, S.-W.; Wei, K.-H.; Sun, Y.-S.; Jeng, U.-S.; Liang, K. S. *Macromolecules* **2005**, *38*, 6559−6565.
(37) Ruokolainen, J.; ten Brinke, G.; Ikkala, O. T. *Adv. Mater.* **1999**, *11*, 777−780.
(38) Bhattacharya, S.; Nayak, S. K.; Chattopadhyay, S.; Banerjee, M.; Mukherjee, A. K. *J. Phys. Chem. A* **2001**, *105*, 9865−9868.
(39) Bhattacharya, S.; Nayak, S. K.; Chattopadhyay, S. K.; Banerjee, M.; Mukherjee, A. K. *Spectrochim. Acta, Part A* **2001**, *57*, 309−313.
(40) Cheng, J.-X.; Fang, Y.; Huang, Q.-J.; Yan, Y.-J.; Li, X.-Y. *Chem. Phys. Lett.* **2000**, *330*, 262−266.
(41) Zhao, Y.; Fang, Y. *J. Phys. Chem. B* **2004**, *108*, 13586−13588.
(42) Ruokolainen, J.; ten Brinke, G.; Ikkala, O.; Torkkeli, M.; Serimaa, R. *Macromolecules* **1996**, *29*, 3409−3415.
(43) Ruokolainen, J.; Torkkeli, M.; Serimaa, R.; Vahvaselkä, S.; Saariaho, M.; ten Brinke, G.; Ikkala, O. *Macromolecules* **1996**, *29*, 6621−6628.
(44) Huh, J.; Ginzburg, V. V.; Balazs, A. C. *Macromolecules* **2000**, *33*, 8085−8096.
(45) Thompson, R. B.; Ginzburg, V. V.; Matsen, M. W.; Balazs, A. C. *Science* **2001**, *292*, 2469−2472.
(46) Thompson, R. B.; Ginzburg, V. V.; Matsen, M. W.; Balazs, A. C. *Macromolecules* **2002**, *35*, 1060−1071.
(47) Yeh, S. W.; Chang, Y. T.; Chou, C. H.; Wei, K. H. *Macromol. Rapid Commun.* **2004**, *25*, 1680−1686.

MA061165G